

Effect of sintering temperature on the structural, morphological and humidity sensing properties of ZnO nanostructure

A. Zaidi^{a,*}, K. Tiwari^a, R. R. Awasthi^b, K. C. Dubey^c

^a*Department of Physics, B.B.D. University, Lucknow-226020, U.P., India*

^b*Faculty of engineering and technology, Khwaja Moinuddin Chisti Language University Lucknow, 226013, U.P., India*

^c*Department of Physics, Shia P. G. College, Lucknow-226003, U.P., India*

ZnO metal oxide powder was prepared using co-precipitation method and the effect of sintering temperature was studied. Powder X-ray diffraction (PXRD) technique has been used to investigate the crystal structure and phase analysis. The wurtzite hexagonal crystal structure of the ZnO powder has been clearly seen in the PXRD pattern. Using the Scherer's formula, the average crystallite size of ZnO powder was determined to be between 27 and 37 nm. The surface has grown spherical nanoparticles with size varying from ~100 nm to ~200 nm, as shown in the scanning electron microscopy (SEM) photograph.

(Received May 6, 2023; Accepted August 2, 2023)

Keywords: ZnO, XRD, SEM, Sintering, Humidity

1. Introduction

Due to their potential applications in functional devices, metal oxide semiconducting nanoscale notably zinc oxide (ZnO), titanium oxide (TiO₂), tin oxide (SnO₂), etc. have attracted a lot of interest recently [1-5]. Because of its non-toxicity and cheap prices, ZnO nanoparticles have grown to be more significant among these metal oxides compared to others. ZnO Nanomaterials are unusual chemical, optical, physical, dielectric, and sensing nanomaterials with wide optical band gap (3.37 eV) and a high exciton binding energy of 60 meV at room temperature. Due to its enormous importance for functional applications, including humidity and gas sensors, optoelectronic devices, solar cells, and many other significant modern uses, ZnO semiconductor has earned a considerable amount of attention. Several research groups have described a variety of approaches for manufacturing nanoparticles [6-15]. Numerous techniques, such as wet chemical methods, physical vapour deposition, metal organic chemical vapour deposition, hydrothermal, pulsed laser deposition, molecular beam epitaxy (MBE), sputtering, electro spinning, etc., have been utilized by the researchers to prepare ZnO nanoparticles [16-26]. Most of these fabrication techniques potentially work at extreme temperatures and necessitate expensive equipment. Furthermore, the artificial synthesis of nanoparticles of metal oxide pollutes the environment and poses a serious danger to human health. Co-precipitation method is a chemical strategy that is chemical technique relatively less expensive in comparison to other methods and effective for resolving the aforementioned issue. It is also non-toxic, cheap, and environmentally benign [27-33]. In the proposed investigation, we examined over how sintering temperature impacted the structural, morphological, and humidity sensing characteristics of ZnO nanostructures manufactured by using co-precipitation technique.

* Corresponding author: anamzaidi623@gmail.com
<https://doi.org/10.15251/JOR.2023.194.411>

2. Experimental section

ZnO nanostructures were prepared in the ongoing research effort using the co-precipitation technique. The deionized water was used to dissolve the zinc acetate $[\text{Zn}(\text{CH}_3\text{COO})_2 \cdot 2\text{H}_2\text{O}]$ before adding few drops of concentrated nitric acid until transparent precursor solution was obtained. On a magnetic stirrer, the precursor solution was continuously stirred for 3 hours resulting in a homogeneous, transparent solution. By adding the suitable amounts of 1N sodium hydroxide (NaOH) in the clear aqueous solution until precursor solutions were precipitated. After that the white precipitate was filtered from mixture and cleaned repeatedly with methanol and purified water to get desired powder. The dry powder was grinded using mortar and pestle and sintered at 450°C , 500°C , 550°C and 600°C for three hours in SiC furnace. The synthesized ZnO powder has been characterized by X-ray diffraction (XRD), using Rigaku Ultima IV, $\text{CuK}\alpha$ ($\sim 1.5406 \text{ \AA}$) and scanning electron microscopy (SEM) using JEOL JSM 7610f with LM. Humidity sensing was measured in well controlled humidity chamber using a typical high precision hygrometer and high sensitive multimeter.

3. Results and discussion

3.1. X-ray diffraction analysis

Figure 1 displays the powder X-ray diffraction (XRD) patterns of ZnO bulk materials sintered at 450°C , 500°C , 550°C and 600°C . The X-ray diffraction pattern of hexagonal wurtzite crystals with the $P6_3mc$ space group is clearly visible in the ZnO bulk sample and well matches with the (JCPDS card No. 75-0576). Yet, ZnO powder X-ray diffraction pattern does not exhibit any additional reflection of impurity peaks, proving that the sample is extremely pure. The polycrystalline hexagonal wurtzite structure of ZnO with $P6_3mc$ space group is revealed by the presence of large diffraction peaks in the sample, such as (100), (002), (101), (102) and (110) planes in X-ray diffraction patterns.

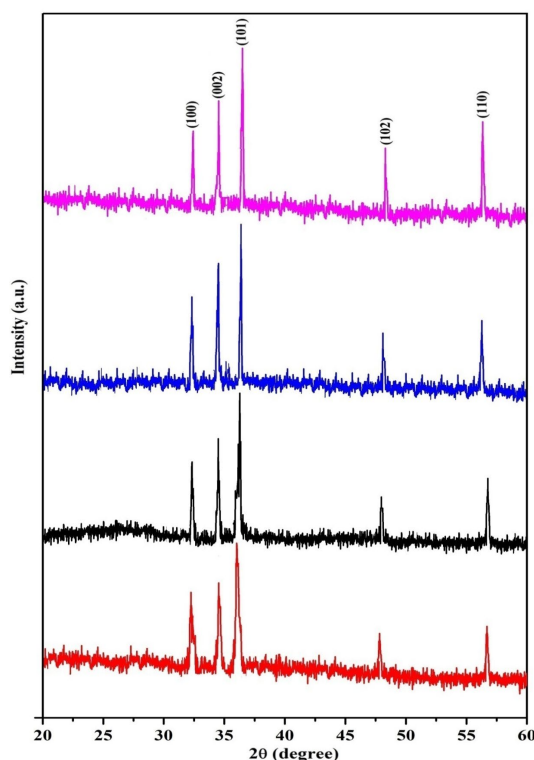


Fig. 1. XRD patterns of ZnO powder sintered at 450°C , 500°C , 550°C and 600°C .

Using the Scherer's formula, the average crystallite size (D) of the samples of ZnO bulk was determined. [20]:

$$D = \frac{K\lambda}{\beta \cos \theta} \quad (1)$$

where K is constant (K=0.9), λ is the X-ray wavelength used in XRD (CuK α 1=1.5406 Å), θ is the Bragg angle; and β is the full-width at half-maximum (FWHM). Using the Scherer's formula, it was determined that the average crystallite size of ZnO nanomaterials sintered at 450 °C, 500 °C, 550 °C and 600 °C and found to be ~27, ~29, ~34 and ~37 nm respectively.

Peak-position (2 θ) which stands for X-ray diffraction wavelength 1.5406 nm, are used to compute the structural properties lattice-constants (a & c) from XRD data.

$$a = \sqrt{\frac{1}{3} \frac{\lambda}{\sin \theta}} \quad (2)$$

$$c = \frac{\lambda}{\sin \theta} \quad (3)$$

The lattice parameters of ZnO thin films unit cell have been calculated using equation 2 & 3 and found to be a = b = 3.0035 Å, c = 5.2048 Å; a = b = 3.0037 Å, c = 5.2049 Å; a = b = 3.0042 Å, c = 5.2052 Å; a = b = 3.0043 Å, c = 5.2053 Å at different sintered at 450 °C, 500 °C, 550 °C and 600 °C respectively.

The volume (V) of hexagonal crystal of ZnO nanostructures can be calculated by following equations,

$$V = \left[\left(\frac{\sqrt{3}}{2} \right) a^2 c \right] \quad (4)$$

where a and c is the lattice parameter of hexagonal crystal of ZnO structures. The volume of ZnO nanostructures' hexagonal unit cell was calculated and found to be 40.66, 40.67, 40.69 and 40.70 Å³ at different sintering temperatures 450 °C, 500 °C, 550 °C and 600 °C respectively. It may be because of an increase in the lattice constant, but the volume of the hexagonal unit cell of ZnO bulk sample also marginally increases with increasing sintering temperature due to increase in the grain size of the sample.

3.2. Scanning electron microscopy analysis

Figure (2a-d) shows the SEM micrographs of ZnO bulk materials sintered at 450 °C, 500 °C, 550 °C and 600 °C were observed at constant magnifications. For various sintering temperature, the surface morphology indicates the formation of spherical-shaped nanoparticles with granular textures. The asymmetrical spherical shape nanostructure with high packing density is also clearly seen in the SEM image, which is uniformly dispersed across the sample surface formation.

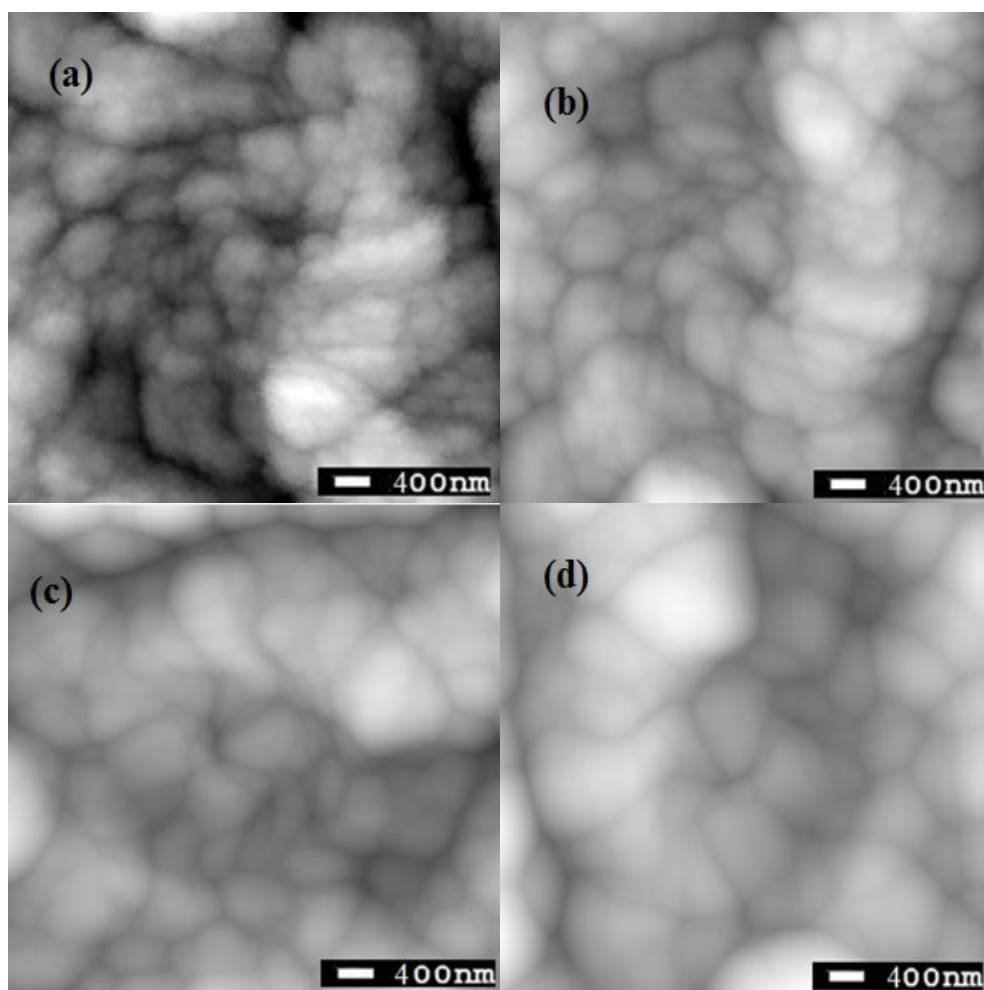


Fig. 2. (a-d) SEM images of ZnO bulk sintered at 450 °C, 500 °C, 550 °C and 600 °C.

The dispersed grains and grain boundaries with particle sizes ranging between ~100 to ~200 nm are seen in the SEM images of ZnO pellet with different sintering temperature. With rising sintering temperature a small increase in particle size was observed and seen in SEM image. Microstructures of ZnO sample shows that the particles are regularly distributed throughout the surface of the pellets, leading to their asymmetrical and uneven spherical shape. The asymmetrical shaped particles that may be seen in SEM images are likely manufactured nanoparticles with a high volume to surface ratio. Furthermore SEM image analysis was performed using Image J (version 1.46r), a piece software. Using Image J software, the observed standard deviations and mean deviations of ZnO bulk pellets were determined to be 36.719, 39.526, 40.523, 42.143 and 126.464, 129.392, 131.321, 132.023 respectively. As a result, the standard deviation showed that pixels were dispersed around the crystallite's mean. The measurement shows that the standard deviation is closest to the median deviation. As a result, the SEM micrograph's instability is expressed as a standard deviation's significance.

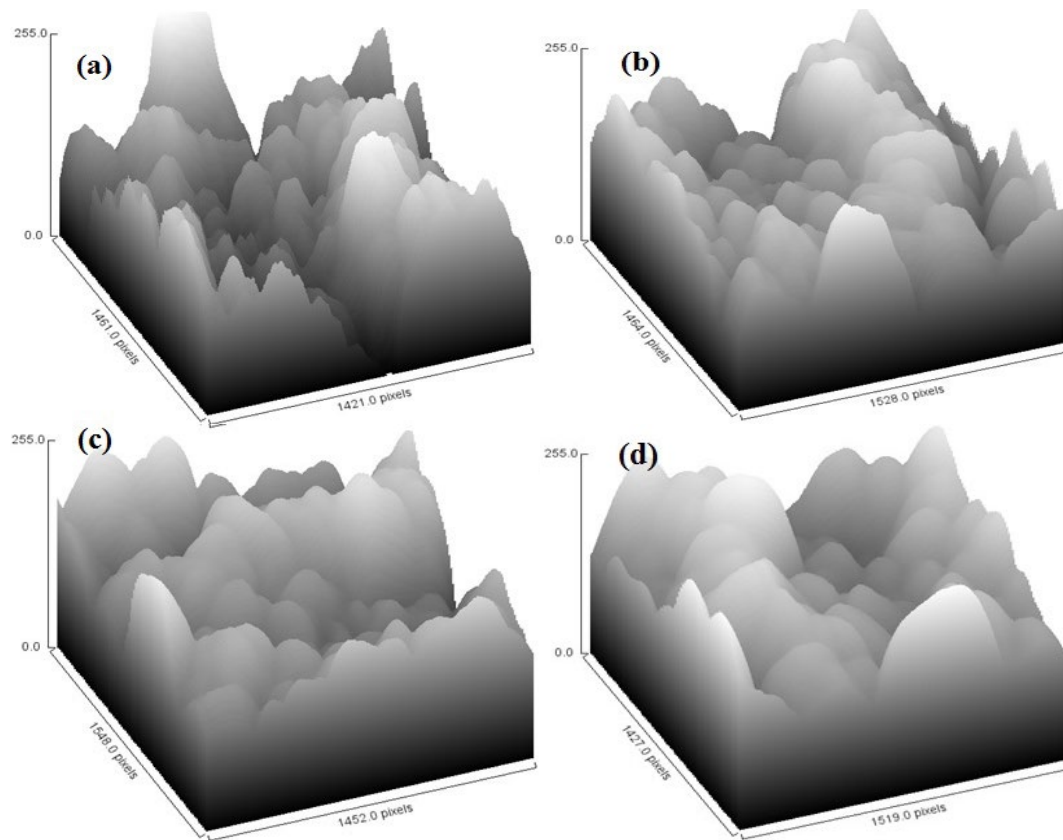


Fig. 3. (a-d) Hill stack surface plot of SEM image of ZnO bulk.

The hill stack surface plot of a SEM image created with Image J is shown in Figure (3a-b). Hill stack surface plot demonstrates improved crystalline ZnO bulk materials performance for sintering temperature values. It is also evident that grain growth of Z direction suppress with increase the sintering temperature from 450 °C to 600 °C.

3.3. Humidity sensing and sensitivity analysis

ZnO powder has been fabricated by co-precipitation technique sintered with varied sintering temperature and humidity sensing characteristics have been studied. Samples were placed in a humidity control chamber for humidity sensing applications, where pure potassium sulphate (K_2SO_4) was utilized as a humidifier and potassium hydroxide (KOH) as a dehumidifier. Resistance changes were seen in accordance with changes in humidity levels. Using a typical hygrometer and sensing materials with varying sintering temperature, as shown in figure 5, the variation of resistance to change in %RH has been measured.

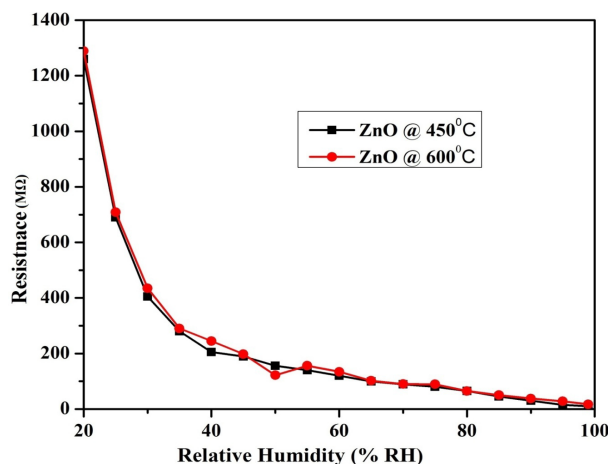


Fig. 4. Variation of resistance of ZnO sample versus change in relative humidity %RH sintered at 450 °C and 600 °C.

It has been observed that resistance constantly decreases when relative humidity increases in the range of (~ 40 %RH), which may be related to the sample's superior conductivity of ZnO powder. The findings of the humidity gas sensing measurements showed that ZnO powder generated at various sintering temperature exhibited quick reaction traits as well as good repeatability. ZnO bulk fashioned at 450 °C and 600 °C sintering temperature demonstrate good sensitivity in the range of 13.50 MΩ/%RH to 14.25 MΩ/%RH, respectively. As a result, produced ZnO bulks have the potential to be applied as humidity gas sensors.

3.4. Aging characteristic of samples

The implementation of sensing mechanism is significantly hindered by the ageing effect of nanoparticles, which is a highly important issue. We examined and noted the attributes of ZnO bulk at 450 °C and 600 °C sintering temperature.

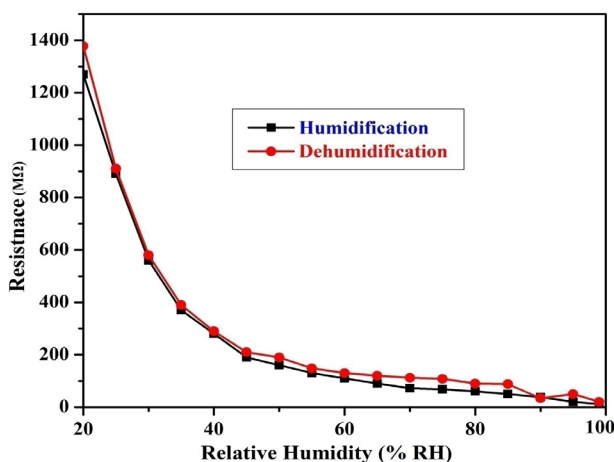


Fig. 5. Aging behavior of ZnO bulk pellet sintered at 450 °C.

After 3 months, the humidity well control chamber was used to study the ageing effect of ZnO bulk. The ageing characteristics of the sample presented in figures 5 and 6 were revealed the variations in resistance versus %RH of ZnO sample. Figure 5's changes of resistance versus %RH demonstrate a small hysteresis loop that is best illustrated by the ZnO bulk sintered at a 450 °C temperature.

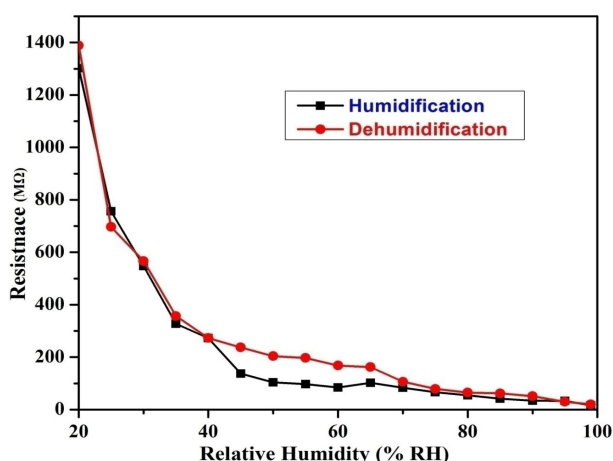


Fig. 6. Aging behavior of ZnO bulk pellet sintered at 600 °C.

However ZnO bulk sintered at a 600 °C no hysteresis loop and substantially less ageing impact, providing good performance for up to 3 months, as shown in figure 6. As a result, it was discovered the sintered at a 450 °C leads to a tuning of the potential application of a humidity gas sensor.

4. Conclusions

ZnO nanoparticles were constructed using the co-precipitation technique in the current study. This process is a low-cost, extremely simple, and reproducible way to create ZnO nanomaterials on a large scale. The powder X-ray diffraction pattern of the prepared samples confirmed the formation hexagonal wurtzite nanomaterial has a crystalline structure. The Scherrer's formula has been used to calculate the average crystalline size, which was found to be in the range between 27 and 37 nm. The SEM image showed spherical-shaped grains that ranged in diameter from ~100 to ~200 nm and were evenly dispersed across the surface. ZnO bulk sintered at different temperature 450 °C and 600 °C have been identified as having excellent humidity sensing properties in the range of 13.50 MΩ/%RH and 14.25 MΩ/%RH, respectively.

Acknowledgements

The authors are thankful to Research and Development plan Government of U.P. India for providing financial support. The authors are highly thankful to Department of Physics, University of Lucknow, Lucknow, for providing the characterization facility.

References

- [1] M. Rai, A. Ingle, *Biotechnol.* 94, 287-293 (2012); <https://doi.org/10.1007/s00253-012-3969-4>
- [2] Geun-Hyoung Lee, *Electronic Materials Letters* 6, 155-159 (2010); <https://doi.org/10.3365/eml.2010.12.155>
- [3] N. Baig, I. Kammakam, W. Falath, *materials. Advances* 2, 1821-1871 (2021); <https://doi.org/10.1039/D0MA00807A>
- [4] J. Yoo, J. Lee, S. Kim, K. Yoon, I. J. Park, S. K. Dhungel B. Karunagaran, D. Mangalaraj and J. Yi, *Thin Solid Films* 213, 480-481 (2005); <https://doi.org/10.1016/j.tsf.2004.11.010>

- [5] K. Keis, C. Bauer, G. Boschloo, A. Hagfeldt, K. Westermark, H. Rensmo and H. Siegbahn, *Photobio. A* 148, 57-64 (2002); [https://doi.org/10.1016/S1010-6030\(02\)00039-4](https://doi.org/10.1016/S1010-6030(02)00039-4)
- [6] J. Carrey, H. Carr'ere, M.L. Kahn, B. Chaudret, X Marie and M Respaud, *Semicond. Sci. Technol.* 23, 025003 (2008); <https://doi.org/10.1088/0268-1242/23/2/025003>
- [7] H.S. Song, W.J. Zhang, C. Cheng, Y.B. Tang, L.B. Luo, X. Chen, C.Y. Luan, X.M. Meng, J.A. Zapien, N. Wang, C.S. Lee, I. Bello, S.T. Lee, *Cryst. Growth Des.* 11, 147-153 (2011); <https://doi.org/10.1021/cg101062e>
- [8] A. H. Battez, R. Gonzalez, J. L. Viesca, J. E. Fernandez, J.M.D. Fernandez, A. MacHado, R. Chou, J. Riba, *Wear* 256, 422-428 (2008).
- [9] F. Porter, *Zinc Handbook Properties, Processing, and Use in Design*, CRC Press. (1991); <https://doi.org/10.1201/9781482276947>
- [10] D. Wu, Z. Bai, K. Jiang, *Materials Letters*, 63, 1057-1060 (2009); <https://doi.org/10.1016/j.matlet.2009.02.008>
- [11] H. Serier, M. Gaudon, M. Me'ne'trier, *Solid State Sci.* 11, 1192-1197 (2009); <https://doi.org/10.1016/j.solidstatesciences.2009.03.007>
- [12] A.F. Lotus, Y.C. Kang, J.I. Walker, R.D. Ramsier, G. G. Chase, *Mater. Sci. Eng. B* 166, 61-66 (2010); <https://doi.org/10.1016/j.mseb.2009.10.001>
- [13] H. Cheng, X. J. Xu, H. H. Hng, J. Ma, *Ceram Int.* 35, 3067-3072 (2009); <https://doi.org/10.1016/j.ceramint.2009.04.010>
- [14] A. Verma, F. Khan, D. Kar, B. C. Chakravarty, S. N. Singh, M. Husain, *Thin Solid Films* 518, 2649-2653 (2010); <https://doi.org/10.1016/j.tsf.2009.08.010>
- [15] E. Hammarberg, A. P. Schwab, C. Feldmann, *J. Colloid Interface Sci.* 334, 29-36 (2009); <https://doi.org/10.1016/j.jcis.2009.03.010>
- [16] T. Ogi, D. Hidayat, F. Iskandar, A. Purwanto, K. Okuyama, *Adv. Powder Technol.* 20, 203-209 (2009); <https://doi.org/10.1016/j.appt.2008.09.002>
- [17] B. D. Ahn, H. S. Kang, J. H. Kim, G. H. Kim, H. W. Chang, S.Y. Lee, *J. Appl. Phys.* 100, 093701(1-6) (2006); <https://doi.org/10.1063/1.2364041>
- [18] R. Brayner, R. Ferrarilliou, N. Brivos, S. Djediat, M. F. Benedetti, F. Fievet, *Nano. Lett.* 6, 866-870 (2006); <https://doi.org/10.1021/nl052326h>
- [19] E. Liu, P. Xiao, J.S. Chen, B.C. Lim, L. Li, *Curr. Appl. Phys.* 8, 408 (2008); <https://doi.org/10.1016/j.cap.2007.10.025>
- [20] P. V. Kamat, B. Patrick, *J. Phys. Chem.* 96, 6829-6834 (1992); <https://doi.org/10.1021/j100195a055>
- [21] S. Du, Y. Tian, H. Liu, J. Liu, Y. Chen, *J. Am. Ceram. Soc.* 89, 2440 (2006); <https://doi.org/10.1111/j.1551-2916.2006.01093.x>
- [22] B. Ismail, M. Abaab, B. Rezig, *Thin Solid Films* 383, 92-94 (2001); [https://doi.org/10.1016/S0040-6090\(00\)01787-9](https://doi.org/10.1016/S0040-6090(00)01787-9)
- [23] L.W. Ji, W.S. Shih, T.H. Fang, C.Z. Wu, S.M. Peng, T.H. Meen, *J. Mater Sci.* 45, 3266-3269 (2010); <https://doi.org/10.1007/s10853-010-4336-4>
- [24] X. Chen, Y. He, Q. Zhang, L. Li, D. Hu, T. Yin, *J. Mater Sci.* 45, 953-960 (2010); <https://doi.org/10.1007/s10853-009-4025-3>
- [25] H. Zhang, D. Yang, S. Li, X. Ma, Y. Ji, J. Xu, D. Que, *Mater. Lett.* 59, 1696-1700 (2005); <https://doi.org/10.1016/j.matlet.2005.01.056>
- [26] W-H Zhang, W-D Zhang, J-F Zhou, *J. Mater Sci.* 45, 209-215 (2010); <https://doi.org/10.1007/s10853-009-3920-y>
- [27] T. Tsubota, M. Ohtaki, K. Eguchi, H. Arai, *J. Mater. Chem.* 7, 85 (1997); <https://doi.org/10.1039/a602506d>
- [28] Y. Zhang, Y. Yang, J. Zhao, R. Tan, W. Wang, P. Cui, W. Song, *J. Mater Sci.* 46, 774-780 (2011); <https://doi.org/10.1007/s10853-010-4813-9>
- [29] S. Anniebell, C.B.S. Gopinath, *Curr. Med. Chem.* 25, 1433-1445 (2018); <https://doi.org/10.2174/0929867324666170116123633>

- [30] P. Kadam, C. Agashe, S. Mahamuni, J. Appl. Phys. 104, 103501 (2008); <https://doi.org/10.1063/1.3020527>
- [31] Y. L. Zhang, Y. Yang, J. Zhao, R. Tan, P. Cui, W. J. Song, J. Sol-Gel Sci. Technol. 51, 198-203 (2009); <https://doi.org/10.1007/s10971-009-1959-5>
- [32] H. X. Chen, J. J. Ding, X. G. Zhao, S. Y. Maa, Physica B. 405, 1339-1344 (2010); <https://doi.org/10.1016/j.physb.2009.11.085>
- [33] N. Wang, Y. Yang, G. Yang. Nanoscale Res. Lett. 6, 338 (2011); <https://doi.org/10.1186/1556-276X-6-338>